Temporal variability of the descent of high-altitude NO_X inferred from ionospheric data

Mark A. Clilverd[1], Annika Seppälä[2], Craig J. Rodger[3], Neil R. Thomson[3], János Lichtenberger[4], and Péter Steinbach[5]

Abstract. In this study we investigate periods of enhanced ionization in the mesosphere during northern hemisphere winter-times. Long-lasting ionization enhancements (days) are typically produced by solar proton events, or by the descent of thermospheric NO_X during periods of sustained downwards vertical transport associated with a strong underlying polar vortex. Using a new application of ground-based low frequency radio wave remote sensing we study the mesospheric ionization conditions during the northern hemisphere winters spanning 2003-04, 2004-05, and 2005-06. The winter 2003-04 subionospheric radio wave propagation data from a transmitter in Iceland shows signatures of the descent of NO_X through 80 km altitude starting on January 13, 2004, during the occurrence of a strong polar vortex, indicating a thermospheric source for the NO_X. Similar analysis of radio wave propagation data in the northern hemisphere winter of 2004-05 does not show a NO_X descent event passing through the mesosphere, due to a lack of downward vertical transport as a result of a weak underlying polar vortex, despite the occurrence of significant solar proton ionization during January 2005. In 2005-06 there were no significant ionization events and also no descent of significant amounts of thermospheric NO_X, despite a strong polar vortex and strong vertical transport. We model the signature of the descent of NO_X seen in the radio wave propagation data using the Sodankylä Ion Chemistry model, confirming that the levels of NO_X in the mesosphere are ~100 times the usual background levels. The combination of strong NO_X sources in the thermosphere and also a strong polar vortex is required for NO_X to descend into the stratosphere with significant concentration levels.

1. Introduction

Winter-time polar odd nitrogen, NO_X ($NO + NO_2$), is produced at high altitudes in the thermosphere and the mesosphere. During periods of efficient vertical transport the NO_X can descend to the stratosphere. In the upper mesosphere the NO_X is mainly in the form of NO. As the NO_X descends below 70 km it is converted to NO_2 [Solomon et al., 1982a; Brasseur and Solomon, 2005]. NO_X plays a key role in the ozone balance of the middle atmosphere because it destroys odd oxygen ($O+O_3$) through catalytic reactions [e.g., Brasseur and Solomon, 2005, pp. 336-355]. Hard energetic particle precipitation (EPP) into the mesosphere (that including a significant population of >100 keV electrons and >1 MeV protons), and softer EPP into the thermosphere (<100 keV electrons), generate in-situ enhancements in odd nitrogen. The mesospheric source is dominated by strong impulsive ionization episodes such as solar proton events [Verronen et al., 2005], while the thermospheric source is more continuous, being dominated by auroral ionization [Siskind, 2000]. During the dark polar winter, odd nitrogen can survive, and in the presence of strong polar vortex conditions, descend into the stratosphere [Solomon et al., 1982a; Siskind, 2000]. During the northern polar winter of 2003-2004 these conditions existed; Randall et al. [2005] reported unprecedented levels of spring-time stratospheric NO_X as a result. Rinsland et al. [2005] also observed very high NO_X mixing ratios at 40-50 km in February/March 2004 with the ACE experiment, detecting levels as high as 1365 ppbv. Randall et al. [2006] presented stratospheric data from 2003-2006, confirming the descent of NO_X in spring 2004, and showing the descent of small amounts of NO_X in the northern polar vortex during the spring of 2006, while none was observed in the spring of 2005.

Although several powerful solar storms occurred at the beginning of the 2003-04 winter period (October and November) the principle source of the NO_X was uncertain because of the breakup of the stratospheric vortex in late December 2003. Clilverd et al. [2006a] used radio wave data to show that the primary source for the NO_X was in the auroral zones in the thermosphere, and not a result of in situ production in the mesosphere. The descent of the NO_X began a few days after the end of the stratospheric warming event at the end of December 2003. In that study it was unclear if the thermospheric reservoir of high-altitude NO_X was generated by the large solar storms several months earlier, or by an accumulation of the effects of smaller storms as suggested by Siskind [2000]. Conversely, Renard et al. [2006] suggested that the source of descending NO_X was from in-situ production at around 60 km caused by electrons of a few hundred keV, due to a geomagnetic storm that occurred on 22-25 January 2004.

One of the few experimental techniques which can probe the ionization at these altitudes uses very low-frequency (VLF) electromagnetic radiation, trapped between the lower ionosphere and the Earth [Barr et al., 2000]. The nature of the received radio waves is largely determined by propagation between these boundaries [e.g., Cummer, 2000], termed "subionospheric propagation". Subionospheric VLF propagation allows remote sensing of the upper atmosphere over large regions; these signals can be received thousands of kilometers from the source, where ionospheric modifications lead to changes in the received amplitude and phase. Man-made VLF transmitters provide a well defined modeling situation, due to the known transmitter-receiver locations and fixed frequency operation, generally operating near constantly [Barr et al., 2000]. By using multiple VLF communication transmitters we have previously gained good understanding of the daytime lower ionosphere [Thomson, 1993] and variations during transient changes (e.g., solar flares [Thomson et al., 2005], low-medium energy electron precipitation [Rodger et al., 2005], and solar proton precipitation [Clilverd et al., 2005]).

In this study we analyze ground-based ionospheric data from mid-high latitudes during the northern polar winters of 2003-2004, 2004-2005, and 2005-2006. Subionospheric VLF radio wave propagation is sensitive to ionization located below about 90 km, including that produced by the ionization of NO_X by Lyman-α [Solomon et al., 1982b]. The effect of increased ionization on the propagating signals can be seen as either an increase or decrease in signal amplitude or phase depending on the modal mixture of each signal observed. Given the dynamic behavior of the polar vortex, and the mixing that occurs in it during the winter months, it is reasonable to expect the path integrated radio wave measurements to respond to any large-scale NO_X changes that occur. From the changes in ionospheric propagation conditions during the winter period we determine the levels of mesospheric NO_X either through in situ production or descent from the thermosphere. The three years studied showed significant differences in solar activity, and stratospheric vortex strength, allowing us to study the interplay between these two parameters. We compare the timing of the onset of the radio wave signatures of NO_X in January 2004 with the NO_2 data from GOMOS, which has the advantage over previous satellite observations of the descent of NO_X in being able to measure NO_2 at altitudes up to 70 km, and in the dark polar night conditions well inside the polar vortex.

2. Experimental setup

Here we use narrow band subionospheric LF data from a 37.5 kHz transmitter (call sign NRK, 64ºN, 22ºW, L=5.6) located in Iceland and received at two nearby sites. The receivers are located at: Ny Ålesund, Svalbard (79ºN, 11ºE, L=18.3), and Érd, Budapest (48ºN, 19ºE, L=1.9). These sites are part of the Antarctic-Arctic Radiation-belt Dynamic Deposition VLF Atmospheric Research Konsortia (AARDDVARK). Figure 1 shows the location of the transmitter site (cross), the receiver sites (diamonds), the Sodankylä Ion Chemistry (SIC) modeling location (70°N, 0°E, asterisk), and also indicates the great circle propagation paths between the transmitter and receivers. The dark circle at 60°N indicates an approximate location of the outer edge of the northern polar vortex. This is consistent with the 1700K sPV (potential vorticity) maps shown in Figure 4 of Manney et al. [2005] for a typical strong northern hemisphere upper stratospheric midwinter vortex.

Mesospheric ionization effects on VLF/LF wave propagation can be modeled using the Long Wave Propagation Code [LWPC, Ferguson and Snyder, 1990]. LWPC models VLF signal propagation from any point on Earth to any other point. Given electron density profile parameters for the upper boundary conditions, LWPC calculates the expected amplitude and phase of the VLF signal at the reception point. Thus it can be used to investigate the modification of the ionosphere as long as the induced changes to the electron density altitude-profiles are known. To provide this the Sodankylä Ion Chemistry model [SIC, version 6.8, Verronen et al., 2005] was used to determine the effects of the ionization of descending NO_X on the mesospheric electron density profiles. The combination of LWPC and the SIC model to understand VLF observations has been reported in previous studies [e.g., Clilverd et al., 2005; 2006b].

In this paper we use NO_2 measurements from the GOMOS stellar occultation instrument [Bertaux et al., 2000; Bertaux et al., 2004; Kyrola et al., 2004] on board the Envisat satellite to investigate the timing of the onset of the radio wave signatures of NO_X in January 2004. GOMOS has the advantage over previous satellite observations of the descent of NO_X into the stratosphere in being able to measure NO_2 at altitudes up to 70 km [Hauchecorne et al., 2005], and in the dark polar night conditions well inside the polar vortex [Bracher et al., 2005; Hauchecorne et al., 2007]. The timing of the onset of the descent of NO_X is important in defining the production mechanism, and high altitude observations also help clarify at which altitude it occurs. The GOMOS NO_2 measurements presented here are from the period January-February 2004. For this study we use only GOMOS dark limb (night-time) measurements from the Northern Hemisphere (GOMOS ground processing prototype, GOPR, version 6.0c) from occultations where the star temperature was ≥ 6000 K for the optimal signal-to-noise ratio for data inversion at upper stratospheric and mesospheric altitudes. In the current analysis we have included over 1800 GOMOS occultations from which nearly 1000 are from star 1 (Sirius, magnitude -1.44) and star 23 (21 Eps CMa, magnitude 1.5), and nearly 200 are from star 7 (19Bet Ori, magnitude 0.1). To improve both spatial and temporal coverage we have also included some stars with weaker magnitudes, for the latitudes from 65ºN to 90ºN the overall range of magnitudes is -1.44 to 2.58, while for 55ºN-65ºN it is 1.50 to 3.03. Night-time measurements of NO_2 are a good tracer for NO_X in the stratosphere and the lower mesosphere, but not at higher altitudes where NO_X is mainly in the form of NO [Brasseur and Solomon, 2005].

3. Northern hemisphere winter conditions (2003-2006)

The winter of 2003-2004 was notable because of the unusually high strength of the upper stratospheric vortex in the period from mid-January 2004 to mid-March [Manney et al., 2005]. The stratospheric vortex allows mesospheric air to descend deep into the stratosphere during the polar night [Russell et al., 1993]. In 2003 the upper stratospheric vortex was apparent from the beginning of October, but was disrupted by a stratospheric warming event, reducing downward vertical transport, which lasted from 20 December 2003 to 10 January 2004. In our study all polar vortex dynamics observations are drawn from the NOAA stratospheric products website [http://www.cpc.ncep.noaa.gov/products/stratosphere/]. We make use of the zonal mean temperatures at 2 mb (~45 km altitude) to determine the timing and approximate intensity of the vortex dynamics in the upper stratosphere. In contrast with winter 2003-2004, in winter 2004-2005 the upper stratospheric vortex became less intense at the end of December 2004 and did not recover. The upper stratospheric vortex during the winter of 2005-2006 was similar in many respects to winter 2003-2004, in that an upper stratospheric warming event occurred in January, followed by a return to typical wintertime vortex conditions in February and March 2006.

Solar proton precipitation can produce high levels of NO_X directly into the mesosphere and upper stratosphere because of the high proton particle energies which can penetrate deep into the atmosphere [see Seppälä et al, 2006, Figure 1, for a plot of atmospheric ionization rate from proton precipitation]. In winter 2003-2004 there was a large solar proton event (SPE) in late October 2003, followed by 4 smaller ones through November and December. In winter 2004-2005 there were two small SPEs in November 2004, followed by a large SPE in January 2005. In winter 2005-2006 no SPEs occurred.

High geomagnetic activity produces high levels of NO_X through electron precipitation occurring at auroral altitudes (~120 km) and in some cases in situ in the mesosphere. In winter 2003-2004 there were 10 geomagnetic storms where the daily average K_p was greater than 4 in the 4-month period spanning 1 October to 31 January. A high proportion (8) of these occurred before the end of December. In winter 2004-

2005 there were 7 large geomagnetic storms, although most (4) occurred in January. In contrast, over winter 2005-2006 there were no large geomagnetic storms. Siskind [2000] used 4-month average A_p to describe geomagnetic activity effects on high-altitude NO_X production. The average A_p between 1 October and 31 January ($<A_p>$) during the 2003-04 winter was 22.7, in winter 2004-2005 it was 17.3, and in winter 2005-2006 it was 6.9. The results of Siskind [2000] suggest that $<A_p>$ ~10 is the lower threshold value above which significant concentrations of descending NO_X are likely to be observed within the southern hemisphere polar vortex. We note that the level of $<A_p>$ ~10 is our interpretation of the Siskind [2000] results.

In summary, the two winters with strong polar vortex conditions (2003-2004 and 2005-2006) have very different levels of solar and geomagnetic activity. Winter 2004-2005 has some periods of high geomagnetic activity, but differs in comparison with the other two winters in that it has weak polar vortex conditions after December.

4. Winter-time mesospheric NO_X impact on radio wave observations, 2003-2006

The amplitude difference between midday and midnight for the NRK (Iceland) radio wave signal received at Ny Ålesund has been shown to be sensitive to changes in ionization conditions caused by the descent of NO_X through VLF reflection heights, due to the production of additional ionization from solar Lyman-α radiation (and geo-coronal Lyman-α at night) which ionizes NO at altitudes of 65-95 km. [Clilverd et al., 2006a]. The effect of increased ionization on the propagating signals can be seen as either an increase or decrease in signal amplitude or phase depending on the modal mixture of the signal observed. The quiet day curve (QDC) exhibits around 7-8 dB lower amplitudes during the daylight hours (09-18 UT) than during the night, because of differences in the effective reflection height of the oblique-incidence radio waves and the effective electron density gradient with altitude at the reflection height.

In Figure 2 we plot the variation of the NRK amplitude difference (i.e., the difference between the midday amplitude value and the midnight amplitude in dB each day) for the winters of 2003-04, 2004-05, and 2005-06, with the plot starting at 01 October in each case, and day 1 = 01 January. The plots show periods where the difference amplitude is -8 dB, which is the value expected under normal quiet day curve (QDC) propagation conditions, and represented by a dot-dashed horizontal line. Vertical solid lines represent the times of known solar proton events (SPE) with the peak particle flux units (pfu) given in parentheses plotted close to the vertical solid lines. Vertical dotted lines indicate periods of subionospherically-observed increased ionization conditions, which do not correspond to SPE periods.

As was discussed in Clilverd et al. [2006a] the winter 2003-04 was marked by several large solar proton events in the early winter period, followed by the descent of NO_X into the mesosphere from the thermosphere on January 13, 2004 (day 13 in Figure 2, top panel). This date coincides with the end of the warming event in the upper stratosphere and the beginning of a period with a strong polar upper stratospheric vortex [NOAA website] leading to strong downward vertical transport [Solomon, 1982a]. Enhanced ionization levels in the mesosphere detected through our subionospheric propagation measurements ended about February 19, 2004, lasting for 37 days in total. A less clear enhancement of mesospheric ionization occurred in October, 2003, where an increased difference amplitude was briefly observed, but quickly swamped by the large SPEs that occurred a few days later. We note here that the ionization increases from SPEs can be so large that they dominate the generation of ionization produced by the ionization of descending NO_X, hence masking its detection through our technique.

In winter 2004-05 there were several notable SPEs, but no clear signature of the descent of NO_X into the mesosphere. In contrast to the previous winter the strong polar vortex was weak in January-March 2005, and thus no strong downward vertical transport of NO_X occurred. Two periods of subionospherically detected enhanced ionization, not associated with SPEs, are indicated by vertical dotted lines in the panel, one occurring in early December, 2004, and the other at the end of January, 2005. Both are short-lived (~5 days), and do not show the expected signature of significant NO_X descent, in that the timescales are relatively short and not the ~30 days as observed previously. It is possible that the enhanced ionization at the end of January 2005 is due to the descent of thermospheric NO_X, generated by the previous period of high geomagnetic activity, although there is no evidence for this in ACE data shown Fig. 1 in Randall et al. [2006], and downward vertical transport was unlikely to be significant because the underlying upper stratospheric vortex was not strong at this time.

In winter 2005-2006 no signatures of SPEs or other enhanced ionization periods were observed in the data, despite a strong polar vortex and downward vertical transport after January 25, 2006, lasting more than a month. This indicates that although strong downward vertical transport was present, the sources of NO_X in the thermosphere and mesosphere were too small to produce significant ionization enhancements at the altitudes probed by VLF propagation. As the average A_p in the 4-month winter period was 6 this observation is consistent with the threshold of >10 for observable NO_X descending to 45 km, indicated by the results of Siskind [2000].

The contrast between the three winter periods (2003-06) shows a highly variable source of NO_X in the thermosphere and mesosphere, due to particle precipitation. The appearance of NO_X in the stratosphere, from these high altitude sources, is further controlled by the presence of a strong polar vortex. ACE observations of NO_2 during these three winters show that no NO_2 was observed descending in to the stratosphere in spring 2005, and only a small amount was observed in spring 2006 [Randall et al., 2006]. The results presented in this paper are consistent with those observations. Only when both source and transport are present will significant amounts of NO_X descend into the stratosphere.

5. Modeling NO_X in the mesosphere

In order to model the effect of descending NO_X on the ionization levels as detected through radio wave propagation we employ the SIC model with varying NO_X levels. The resultant electron density profiles are input into the Long Wave Propagation Code (LWPC) following the approach described by Clilverd et al. [2005, 2006b]. Changes in NO_X are modeled by arbitrarily increasing the normal NO profile at a given altitude by factors of 10 - 1000. Figure 3 shows the effect on the electron density profile of a 15 km altitude-limited slab in which there is a 100 times enhancement of NO. The figure shows the effects of the slab centered on 90 km and 70 km, in comparison with the midday and midnight electron density profiles calculated with the SIC model. In all cases a low level proton flux is included in the SIC model runs to provide realistic non-disturbed conditions. At heights above ~70 km, the electron densities in the region of the NO enhancement are increased by a factor of 10, which is consistent with the earlier conclusions of Clilverd et al. [2006a] concerning periods of enhanced ionization due to NO_X transport during the 2003-2004 winter. However at altitudes lower than ~70 km the NO_X enhancement leads to no significant increase in electron density levels because most of the Lyman-α is absorbed at altitudes above the slab height.

Figure 4 shows the LWPC-calculated diurnal changes in the amplitude received from the NRK transmitter at Ny Ålesund, caused by the SIC-modeled NO_X descent for January conditions. The electron density changes due to the NO enhancements have been represented in the LWPC model by exponential profile fits restricted over the altitude range 30-110 km [Wait and Spies, 1964], applied over the entire transmitter-receiver great circle path. In Figure 4 the nighttime amplitudes (00-08 UT, and 18-24 UT) are generally reduced as a result of the enhanced NO, while daytime amplitudes (09-17 UT) increase. The model results shown represent increases of NO by a factor of 10, 100, 300, and 1000 at 80 km altitudes. The plot shows that the nighttime amplitudes decrease with limited sensitivity to the absolute NO enhancement factor, but the daytime amplitudes change consistently with NO enhancement factor.

In Figure 5 we show the QDC from data recorded prior to, and just after, the NO descent period (solid line), as well as the average amplitude during descent period (16-20 January 2004, dashed line). Modeling results from SIC/LWPC are shown by diamonds (QDC, 1×NO), and asterisks (300×NO). As the observed QDC amplitudes are un-calibrated they have been adjusted to the same level as the SIC/LWPC QDC levels which were arbitrarily based on a transmitter output power of 200 kW. We use 200 kW as the exact output power of the NRK transmitter is unknown to us. The 1×NO results agree well with the QDC propagation conditions observed in the data, while the 300×NO increase occurring at 80 km altitude produces behavior similar to that observed in the NRK data during the NO_X descent period starting on January 13, 2004, i.e., a 3 dB decrease during the nighttime and higher daytime amplitudes than during nighttime, giving a day-night difference amplitude of +2.5 dB. Clearly the modeling indicates that the effect of increased NO is detectable on both the nighttime and the daytime radio wave data. In Figure 2 we plot the day-night difference, although we note here that it is possible to plot either day or night individually and still observe the effect. Plotting the day-night difference increases the NO effect on the data, however occasionally operational constraints only allows data collection at either one or the other – this is the case in the data used for section 6 below.

Figure 6 shows the change in day-night difference amplitude as the NO enhancement descends in altitude from 95 to 65 km with 5 km resolution steps. The plot shows the variation for three levels of NO enhancement – 10×NO, 100×NO, and 1000×NO, where 1×NO is the SIC model value for the model location, time of year, and time of day. SIC/LWPC results show that because the day-night difference peaks at 80 km the radio waves are primarily sensitive to the NO_X enhancement as it passes through ~80 km, with little impact on the diurnal variation in amplitude once the NO_X reaches 65 km and below. Hence the subionospheric propagation is sensitive to the early stages of NO_X descent, and can also signal the end of a NO_X descent period, but only if the NO_X changes are significant, i.e., factor of ~10 changes. Satellite-based techniques tend to identify NO_X enhancements at altitudes below 65 km [e.g., Randall et al., 2005; Rinsland et al., 2005]. Subionospheric VLF propagation therefore provides significant additional lead times, detecting NO_X enhancements which are transported to the stratosphere ~6 weeks later.

6. Latitudinal extent of NO_X descent

Up to this point we have shown the effects of the descent of NO_X on the Iceland to Svalbard path (NRK to Ny Ålesund). This path is well inside the usual coverage of the polar vortex. In Figure 7 we show the variation of the 2003-04 winter-time average nighttime amplitude for the Iceland to Hungary path (NRK to Érd) in comparison with the NRK to Ny Ålesund difference amplitude for the same period. We use only nighttime data from Erd because of limited daytime recordings made during this period. However as shown previously in Figure 5 and 6 the nighttime-only data is sensitive to increased NO_X. On the NRK to Érd path the location of the transmitter represents the highest latitude that could be affected by descending NO_X, i.e., 64°N. The plot shows that the Erd nighttime amplitude responds to both SPEs and the descent of NO_X. The horizontal and vertical lines are as Figure 2, with the addition of long-dashed vertical lines showing the end of the descent of NO_X in February 2004. The solar proton events of October/November 2003 show up clearly as short-lived (days) increases in nighttime amplitude of ~7 dB.

The descent of NO_X in January 2004, is also observed on this lower latitude path, possibly starting intermittently on January 6, 2004, and clearly by 12 January, lasting 42 days, but finishing prior to the end of the NO_X-produced enhanced ionization observed on the higher latitude path. This suggests that either downward vertical transport begins ~7 days earlier at lower latitudes, and finishes earlier by ~2 days, or that the outer regions of the polar vortex have faster descent rates than the inner regions – detailed analysis of the dynamics of the outer edge of the polar vortex is beyond the scope of this study, however, we note that this interpretation is consistent with Callaghan and Salby [2002] who show that the maximum descent rate in the polar vortex is not over the pole, but at 60ºN. A recovery of the Érd nighttime amplitudes occurred during early February 2004 (about day 40) suggesting that the downward transport faltered in the lower latitude sector during this time.

These observations indicate that strong downward vertical transport occurs significantly equator-wards of 64°N, increasing the ionization levels on at least part of the path to Érd. Clilverd et al. [2006b] showed that changes in ionization over the first 500 km of this path caused by SPEs were able to produce significant changes in received signal amplitude at Érd. SIC/LWPC model runs [not shown] with 100×NO at 80 km altitude applied to the first 500 km of the path are able to produce the changes observed in Figure 7, i.e., the NO descent also occurs equator-wards of 64°N, which is consistent with previous satellite observations [Randall et al. 2006].

GOMOS observations of NO_2 in January and February 2004 are shown in Figure 8. The observations are averaged over two days to provide the results presented. The left-most panels show the NO_2 zonal mean number density and mixing ratios for latitudes >65°N. The right-most panels show the NO_2 zonal mean number density and mixing ratios for latitudes 55°-65°N. Enhanced levels of NO_2 are seen descending from about 70 km starting on January 10, 2004, reaching altitudes of 45 km by the end of February 2004. Each averaged data point is formed from 15-30 measurements, only a small number of points have less than 15 measurements. Our key conclusions from the GOMOS data (Figure 8 left) are based on nearly 500 occultations of Sirius, which is considered the best star used in GOMOS occultations, providing excellent signal-to-noise for the measurement of NO_2.

The descending NO_2 enhancement is about 100 times that of the background density, and thus shows consistency with the radio wave modeling undertaken above. The enhancement passes below 60 km in early-February, at which time the modeling results indicate that the signature of the NO_X descent should have ceased in the radio wave data. However, a further increase in NO_2 at altitudes >60 km occurs as a result of particle precipitation during the geomagnetic storm of 11-15 February, 2004. The NO_2 eventually descends below 60 km completely after 19 February, consistent with the radio wave observations.

In the right-most panels, representing lower latitude GOMOS observations (55°-65°N), similar signatures of descent of enhanced NO_2 can be seen during January and February, 2004. However, contrary to the radio wave observations from Érd there is no clear signature of the 11-15 February 2004 geomagnetic storm in the GOMOS data, suggesting that the radio wave propagation data is responding more sensitively to a lower latitude source of ionization that is not associated with the enhancement of significant levels of NO_2. Additionally there is no clearly observable onset date with which to confirm the NO_X descent start date of 5 Jan 2004 suggested by the radio wave data, primarily because of a weaker descent feature in these lower latitude measurements.

In Figure 8 we plot the GOMOS data up to an altitude of 70 km. Even using the brightest stars GOMOS is only able to measure NO_2 from 20-70 km. Outside these altitude ranges GOMOS NO_2 data has to be considered with caution [Hauchecorne et al., 2005]. Figure 8 indicates that the descent of NO_2 began around 10 January 2004, about 2 weeks before the geomagnetic storm suggested by Renard et al. [2006] as the cause of the lower mesospheric NO_2 enhancement. In fact GOMOS data indicates that the 22-23 January 2004 geomagnetic storm created no observable enhancement of NO_2 in the 50-70 km altitude range. In contrast the storm of 11-12 February 2004 can be seen to produce significant amounts of NO_2 below 70 km, contributing to the body of NO_2 descending into the stratosphere. The solar wind speed and density increased more markedly during the 11 February storm than the 22 January storm, which is consistent with the enhanced production of NO_X by particle precipitation [e.g., Rozanov et al., 2005]. The gradual increase in NO_2 number density from 10 January to 20 January at altitudes of about 65 km is consistent with the increasingly effective conversion of the descending NO to NO_2 at altitudes below 70 km through reaction with atomic oxygen [Brasseur and Solomon, 2005]. These observations argue strongly against the interpretation of Renard et al. [2006] where the source of descending NO_X was suggested to come from in-situ production at around 60 km caused by electrons of a few hundred keV, due to a geomagnetic storm that occurred on 22-25 January 2004.

7. Discussion and Summary

In this study we have investigated periods of enhanced ionization in the mesosphere during northern hemisphere winter-times. Ionization enhancements lasting days are typically produced by solar proton events. In contrast, ionization enhancements lasting weeks are caused by the descent of thermospheric NO_X during periods of sustained downwards vertical transport associated with a strong underlying polar vortex.

Using a new application of a well established radio wave propagation technique, we have shown that only during winters with both high geomagnetic activity (4-monthly mean A_p>10) and strong downward vertical transport, will large enhancements of polar NO_X be transported down to the stratosphere. These conditions were met in winter 2003-2004, but not in 2004-2005, or 2005-2006 as only high geomagnetic activity or strong downward transport occurred, but not both simultaneously.

In winter 2003-2004 the descent of polar NO_X began on 13 January 2004, a few days after the onset of strong downward transport associated with a strong underlying upper stratospheric polar vortex. The start date is not associated with any specific geomagnetic storm, but rather due to the formation of a strong polar vortex giving rise to strong downward vertical transport of a pre-existing thermospheric reservoir of NO_X. The existence of a significant thermospheric NO_X reservoir is dependent on the average A_p>10 over the preceding 4 months, which agrees with the results of Siskind [2000]. This finding is consistent with the impact of geomagnetically enhanced auroral electron precipitation, leading to a significantly enhanced thermospheric NO_X population in the polar winter.

Both our radio propagation data and independent GOMOS observations indicate significant NO_X descent into the stratosphere from latitudes equator-wards of 65°N. Ground-based measurements made in Hungary indicated that the descent started a few days earlier at lower latitudes than at high latitudes.

The lack of influence of any specific geomagnetic storm argues against an in-situ NO_X production mechanism at altitudes of around 60 km. The results of propagation modeling using the SIC calculations, undertaken to simulate our radio wave observations, are also consistent with a source population descending from >90 km, i.e., auroral altitudes in the thermosphere. This is consistent with previous work indicating that the auroral zone can produce significant quantities of NO_X as a result of geomagnetic disturbances [Baker et al., 2001; Barth 2003]

Acknowledgments. The authors would like to thank Frank Skogen of the Kings Bay Company for overseeing the collection and return of the Ny Ålesund data. We would also like to thank the GOMOS team for their useful and informative discussions regarding this work.

References

Baker, D. N., C. A. Barth, K. E. Mankoff, S. G. Kanekal, S. G. Bailey, G. M. Mason, and J. E. Mazur (2001), Relationships between precipitating auroral zone electrons and lower thermospheric nitric oxide densities: 1998-2000, *J. Geophys. Res.*, 106, 24465-24480.

Barr, R., D. L. Jones, and C. J. Rodger (2000), ELF and VLF Radio Waves, *J. Atmos. Sol. Terr. Phys.*, 62(17-18), 1689-1718.

Barth, C. A., K. D. Mankoff, S. M. Bailey, and S. C. Solomon, Global observations of nitric oxide in the thermosphere, *J. Geophys. Res.*, 108, 1027, doi:10.1029/2002JA009458.

Bertaux, J. L., E. Kyrölä, and T. Wehr (2000), Stellar occultation technique for atmospheric ozone monitoring: GOMOS on Envisat, *Earth Observation Quarterly*, 67, 17-20.

Bertaux, J. L., et al. (2004), First results on GOMOS/Envisat, *Adv. Space Res.*, 33, 1029-1035.

Brasseur, G., and S. Solomon (2005), *Aeronomy of the Middle Atmosphere*, third ed., D. Reidel Publishing Company, Dordrecht.

Bracher, A., et al. (2005), Cross comparisons of O3 and NO2 measured by the atmospheric ENVISAT instruments GOMOS, MIPAS, and SCIAMACHY, Advances in Space Research, Volume 36, Issue 5, p. 855-867, doi: 10.1016/j.asr.2005.04.005.

Callaghan, P. F., and M. L. Salby (2002), Three-dimensionality and forcing of the Brewer-Dobson circulation, J. Atmospheric Sciences, 59, 976-991.

Clilverd, M. A., C. J. Rodger, T. Ulich, A. Seppälä, E. Turunen, A. Botman, and N. R. Thomson (2005), Modeling a large solar proton event in the southern polar atmosphere, *J. Geophys. Res.*, 110, A09307, doi:10.1029/2004JA010922.

Clilverd, M. A., A. Seppälä, C. J. Rodger, P. T. Verronen, and N. R. Thomson (2006a), Ionospheric evidence of thermosphere-to-stratosphere descent of polar NO_X, *Geophys. Res. Lett.*, 33, L19811, doi: 10.1029/2006GL026727.

Clilverd, M. A., A. Seppälä, C. J. Rodger, N. R. Thomson, P. T. Verronen, E. Turunen, Th. Ulich, J. Lichtenberger, and P. Steinbach (2006b), Modeling polar ionospheric effects during the October-November 2003 solar proton events, *Radio Sci.*, 41, RS2001, doi:10.1029/2005RS003290.

Cummer, S. A. (2000), Modeling electromagnetic propagation in the earth-ionosphere waveguide, *IEEE Transactions on Antennas and Propagation*, 48(9), 1420-1429.

Ferguson, J. A., and F. P. Snyder (1990), Computer programs for assessment of long wavelength radio communications, Tech. Doc. 1773, Natl. Ocean Syst. Cent., San Diego, California.

Hauchecorne, A., et al. (2005), First simultaneous global measurements of nighttime stratospheric NO2 and NO3 observed by Global Ozone Monitoring by Occultation of Stars (GOMOS)/Envisat in 2003, *J. Geophys. Res.,* 110 (D18): Art. No. D18301.

Hauchecorne, A., J.-L. Bertaux, F. Dalaudier, J. M. Russell III, M. G. Mlynczak, E. Kyrölä, and D. Fussen (2007), Large increase of NO_2 in the north polar mesosphere in January–February 2004: Evidence of a dynamical origin from GOMOS/ENVISAT and SABER/TIMED data, *Geophys. Res. Lett.*, 34, L03810, doi:10.1029/2006GL027628.

Kyrölä, E., et al. (2004), GOMOS on Envisat: An overview, Adv. Space Res., 33, 1020-1028.

Manney, G. L., K. Kruger, J. L. Sabutis, S. A. Sena, and S. Pawson (2005), The remarkable 2003-2004 winter and other recent warm winters in the Arctic stratosphere since the late 1990s, *J. Geophys. Res*., 110, D04107, doi:10.1029/2004JD005367.

Randall, C. E., et al. (2005), Stratospheric effects of energetic particle precipitation in 2003–2004, *Geophys. Res. Lett.*, 32, L05802, doi:10.1029/2004GL022003.

Randall, C. E., V, L. Harvey, C. S. Singleton, P. F. Bernarth, C. D. Boone, and J. U. Kozyra (2006), Enhanced NO_X in 2006 linked to strong upper stratospheric Arctic vortex, *Geophys. Res. Lett.*, 33, L18811, doi:10.1029/2006GL027160.

Renard, J-B., P-L. Blelly, Q. Bourgeois, M. Chartier, F. Goutail, and Y. J. Orsolini (2006), Origin of the January–April 2004 increase in stratospheric NO_2 observed in the northern polar latitudes, *Geophys. Res. Lett*., 33, L11801, 10.1029/2005GL025450

Rinsland, C. P., C. Boone, R. Nassar, K. Walker, P. Bernath, J. C. McConnell, and L. Chiou (2005), Atmospheric Chemistry Experiment (ACE) Arctic stratospheric measurements of NO_X during February and March 2004: Impact of intense solar flares, *Geophys. Res. Lett.*, 32, L16S05, doi:10.1029/2005GL022425.

Rodger, C. J., M. A. Clilverd, N. R. Thomson, D. Nunn, and J. Lichtenberger (2005), Global prediction of inner radiation belt energy deposition caused by lightning, *Annales Geophys*., 23(11), 3419-3430.

Rozanov, E., L. Callis, M. Schlesinger, F. Yang, N. Andronova, and V. Zubov (2005), Atmospheric response to NO_y source due to energetic electron precipitation, *Geophys. Res. Lett.*, 32, L14811, doi:10.1029/2005GL023041.

Seppälä, A., P. T. Verronen, V. F. Sofieva, J. Tamminen, E. Kyrölä, C. J. Rodger, M. A. Clilverd (2006), Destruction of the tertiary ozone maximum during a solar *proton event, Geophys. Res. Lett*., 33, L07804, doi:10.1029/2005GL025571.

Siskind, D. E. (2000), On the coupling between the middle and upper atmospheric odd nitrogen, in Atmospheric science across the stratopause, Geophysical Mongraph 123, 101-116.

Solomon S, P.J. Crutzen, R. G. Roble (1982a), Photochemical coupling between the thermosphere and the lower atmosphere .1, Odd nitrogen from 50 to 120 km, *J. Geophys. Res.*, 87, 7206-7220.

Solomon S, G. C. Reid, R. G. Roble, and P.J. Crutzen (1982b), Photochemical coupling between the thermosphere and the lower atmosphere .2, D-region ion chemistry and the winter anomaly, *J. Geophys. Res.*, 87, 7221-7227.

Thomson, N.R. (1993), Experimental daytime VLF ionospheric parameters. *J. Atmos. Terr. Phys.*, 55, 173-184.

Thomson, N.R., C.J. Rodger, and M.A. Clilverd (2005), Large solar flares and their ionospheric D-region enhancements, *J. Geophys. Res.*, vol. 110, A06306, doi:10.1029/2005JA011008.

Verronen, P. T., A. Seppälä, M. A. Clilverd, C. J. Rodger, E. Kyrölä, C. Enell, T. Ulich, and E. Turunen (2005), Diurnal variation of ozone depletion during the October–November 2003 solar proton events, *J. Geophys. Res.*, 110, A09S32, doi:10.1029/2004JA010932.

Wait, J. R., and K. P. Spies (1964), Characteristics of the Earth-ionosphere waveguide for VLF radio waves, NBS Tech. Note 300.

____

[1]M. A. Clilverd, Physical Sciences Division, British Antarctic Survey, High Cross, Madingley Road, Cambridge CB3 0ET, England, U.K. (e-mail: macl@bas.ac.uk)

[2]A. Seppala, Finnish Meteorological Institue, Helsinki, Finland (email: annika.seppala@fmi.fi)

[3]C. J. Rodger and N.R. Thomson, Department of Physics, University of Otago, P.O. Box 56, Dunedin, New Zealand. (email: crodger@physics.otago.ac.nz and n_thomson@physics.otago.ac.nz)

[4]J. Lichtenberger, Space Research Group, Eötvös University, Budapest H 1518, Hungary. (email: spacerg@sas.elte.hu)

[5]P. Steinbach, Research Group for Geoinformatics and Space Sciences, MTA-ELTE, Budapest, Hungary. (email: spacerg@sas.elte.hu)

(Received N x, 2006; N x 27, 2006;
accepted N x, 2007.)

Figure 1. The location of subionospheric propagation paths from Iceland to the AARDDVARK receiver sites at Ny Ålesund, and Érd. The Sodankylä Ion Chemistry (SIC) modeling location is also shown.

Figure 2. The day-night difference amplitudes for the Iceland transmitter (NRK) received at Ny Ålesund (NYA) during three winters. Normal values are indicated by the horizontal dashed line. Times of identified solar proton events are given by solid vertical lines with the peak particle flux units (pfu) are given in parentheses plotted close to the vertical solid lines, while similar behavior with no identified proton event is shown by the vertical dotted lines.

Figure 3. The midday (12 UT, bold line) and midnight (00 UT, lighter line) electron density profiles from SIC showing the effect of enhanced NO centered about 90 km (circles), and 70 km (crosses).

Figure 4. The modeled diurnal amplitude of the Iceland transmitter received at Ny Ålesund, Svalbard, under the influence of 10, 100, 300, 1000 × NO enhancements centered on 80 km altitude, compared with the normal diurnal curve (1xNO).

Figure 5. The diurnal amplitude of the Iceland transmitter received at Ny Ålesund, Svalbard, (solid line) compared with the average amplitude during 16-20 January 2004 (dashed line). SIC/LWPC model results are shown for the QDC (1×NO, diamonds) and for a 300×NO enhancement (asterisks) centered at 80 km.

Figure 6. The winter-time differences in day-night amplitude for the Iceland transmitter (NRK) received at Ny Ålesund (NYA) during the descent of a layer of different enhancement factors (10, 100, and 1000). The 1 x NO case is plotted as a dot-dashed line at -3 dB.

Figure 7. The winter-time average nighttime amplitude for the Iceland transmitter received at Érd, Hungary, during winter–time 2003-04 compared with the NRK to Ny Ålesund difference amplitude for the same period. The horizontal and vertical lines are as Figure 2 where the peak particle flux units (pfu) are given in parentheses plotted close to the vertical solid lines, with the addition of long-dashed vertical lines showing the end of the descent of NO_X in February 2004.

Figure 8. (Left top) The GOMOS nighttime NO_2 number density for latitudes >65°N during the period January and February 2004. (Left bottom) The NO_2 mixing ratio over the same period. (Right top) The NO_2 number density for latitudes 55-65°N from January and February 2004. (Right bottom) The NO_2 mixing ratio over the same period. The nighttime NO_2 measurements are used as an estimation of the total NO_X ($NO + NO_2$).

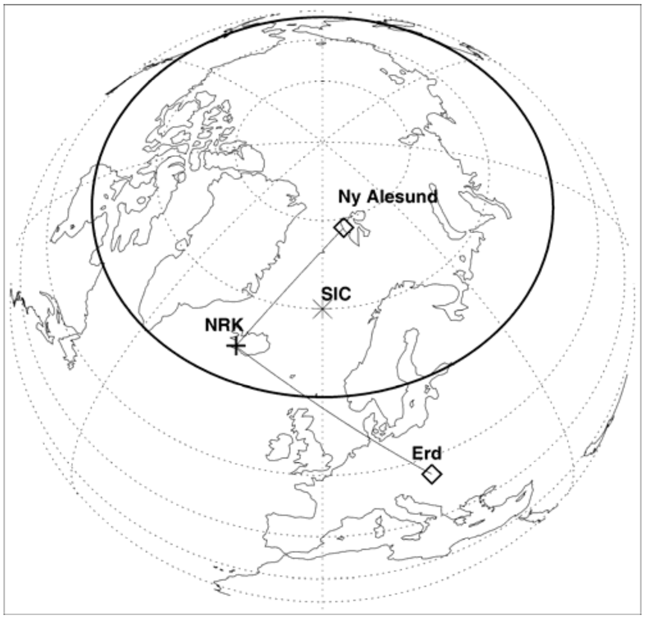

Figure 1. The location of subionospheric propagation paths from Iceland to the AARDDVARK receiver sites at Ny Ålesund, and Érd. The Sodankylä Ion Chemistry (SIC) modeling location is also shown.

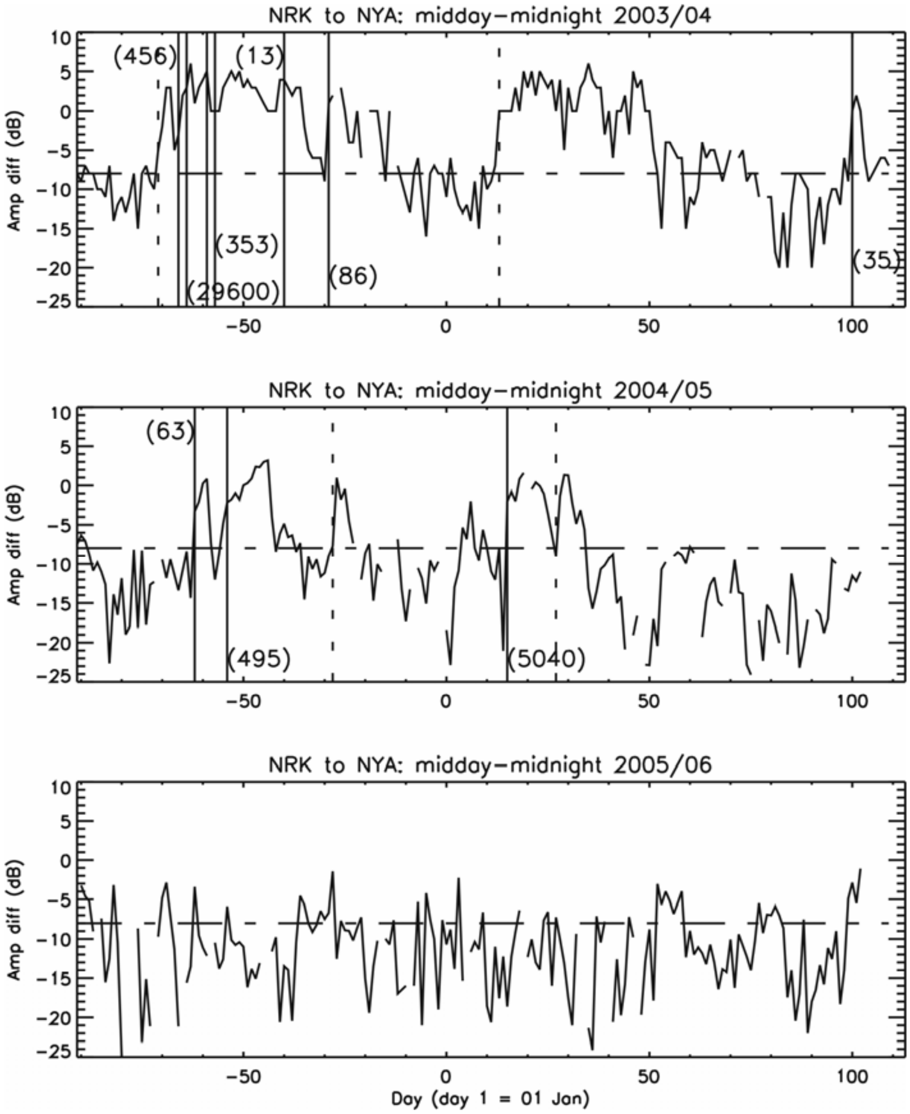

Figure 2. The day-night difference amplitudes for the Iceland transmitter (NRK) received at Ny Ålesund (NYA) during three winters. Normal values are indicated by the horizontal dashed line. Times of identified solar proton events are given by solid vertical lines with the peak particle flux units (pfu) are given in parentheses plotted close to the vertical solid lines, while similar behavior with no identified proton event is shown by the vertical dotted lines.

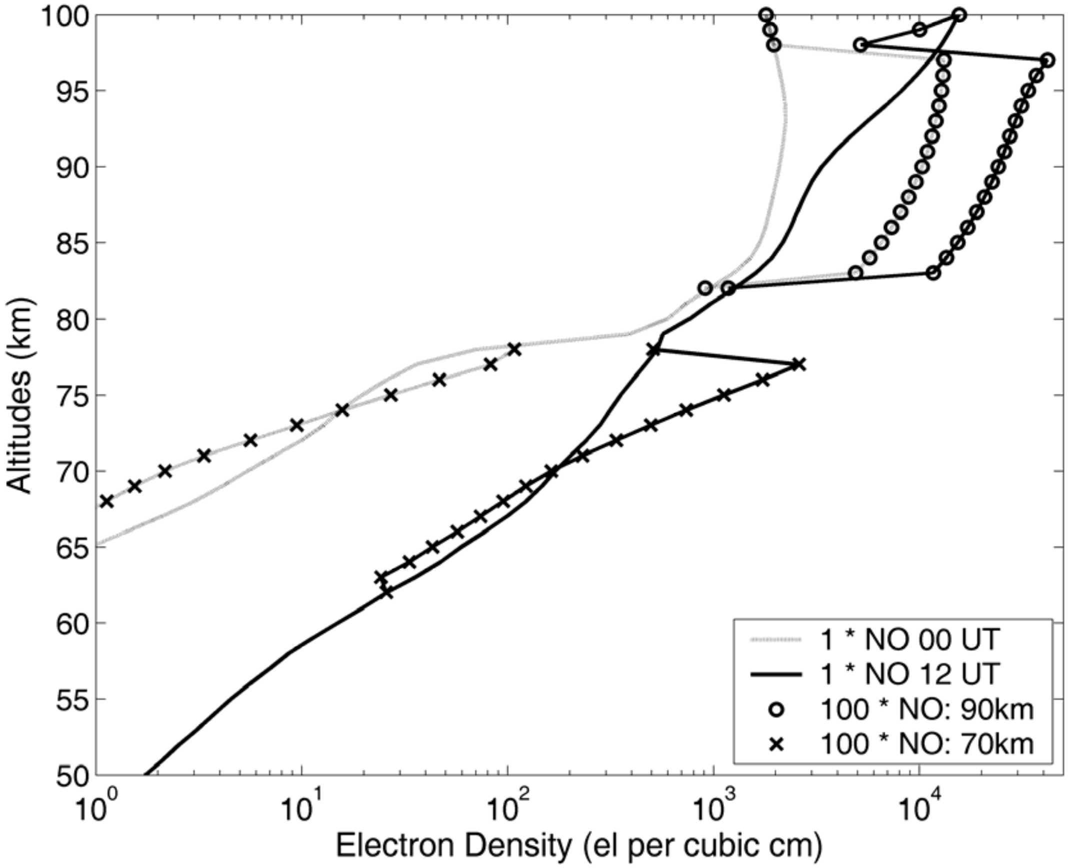

Figure 3. The midday (12 UT, bold line) and midnight (00 UT, lighter line) electron density profiles from SIC showing the effect of enhanced NO centered about 90 km (circles), and 70 km (crosses).

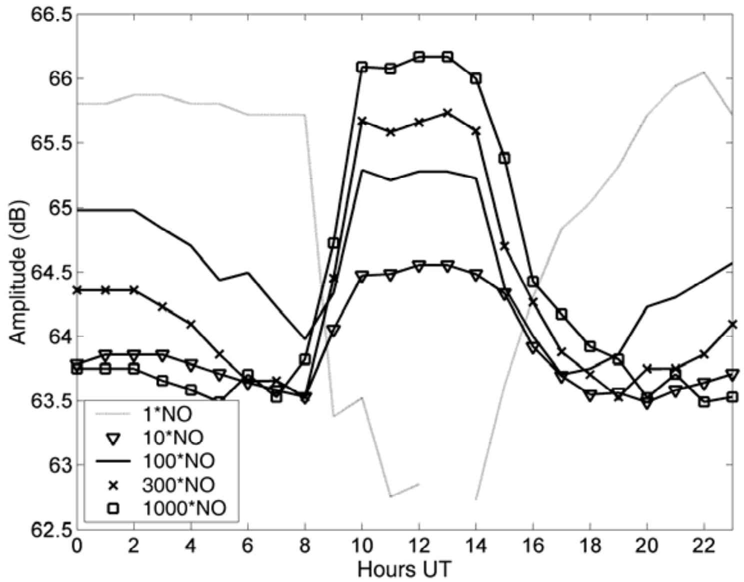

Figure 4. The modeled diurnal amplitude of the Iceland transmitter received at Ny Ålesund, Svalbard, under the influence of 10, 100, 300, 1000 × NO enhancements centered on 80 km altitude, compared with the normal diurnal curve (1xNO).

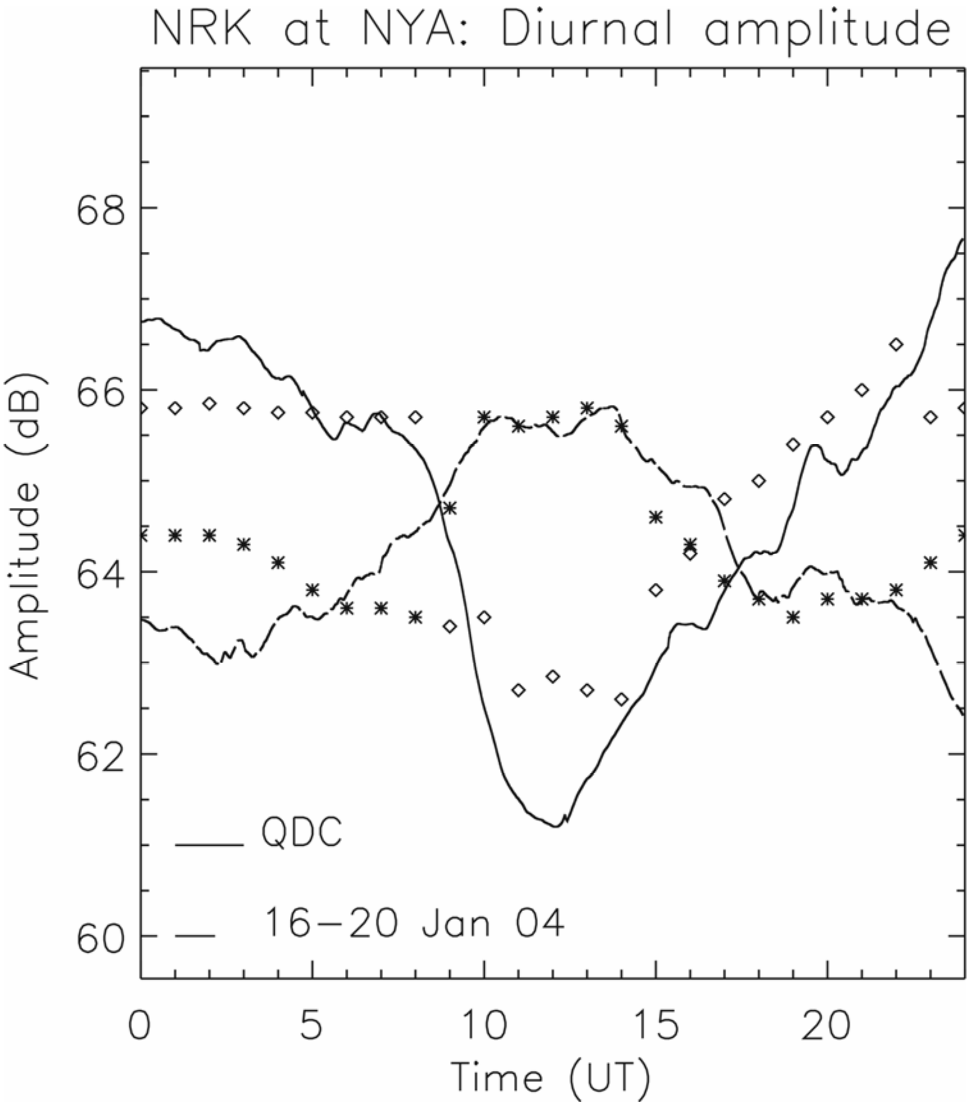

Figure 5. The diurnal amplitude of the Iceland transmitter received at Ny Ålesund, Svalbard, (solid line) compared with the average amplitude during 16-20 January 2004 (dashed line). SIC/LWPC model results are shown for the quiet day curve (QDC, 1×NO, diamonds) and for a 300×NO enhancement (asterisks) centered at 80 km.

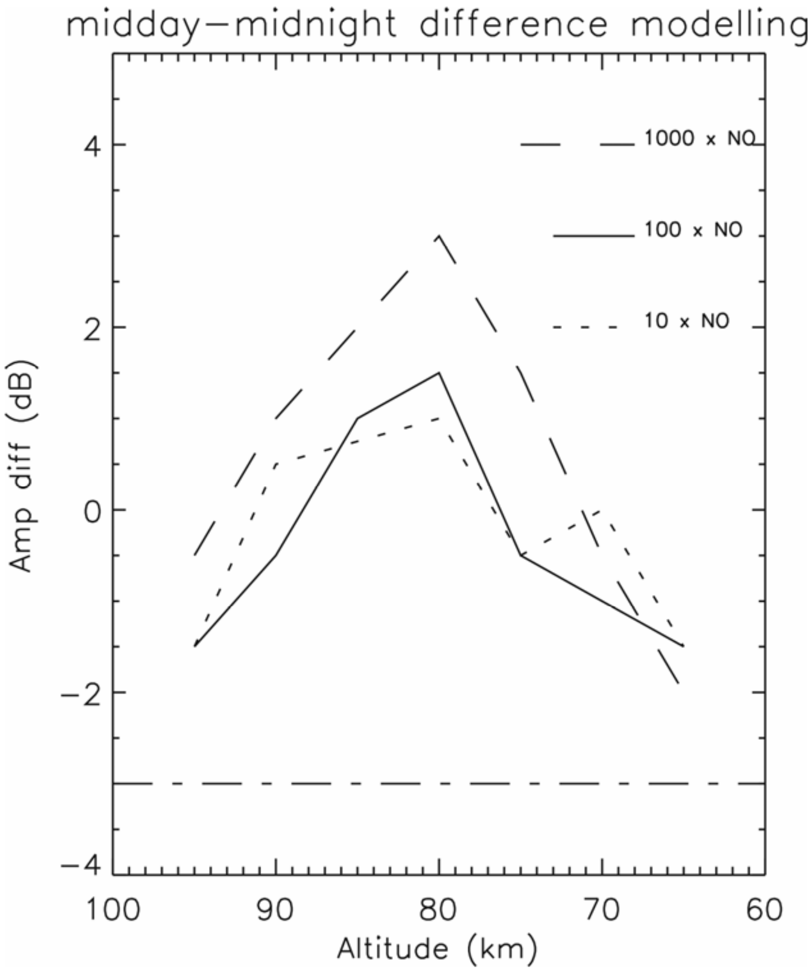

Figure 6. The winter-time differences in day-night amplitude for the Iceland transmitter (NRK) received at Ny Ålesund (NYA) during the descent of a layer of NO with different enhancement factors (10, 100, and 1000). The 1 x NO case is plotted as a dot-dashed line at -3 dB.

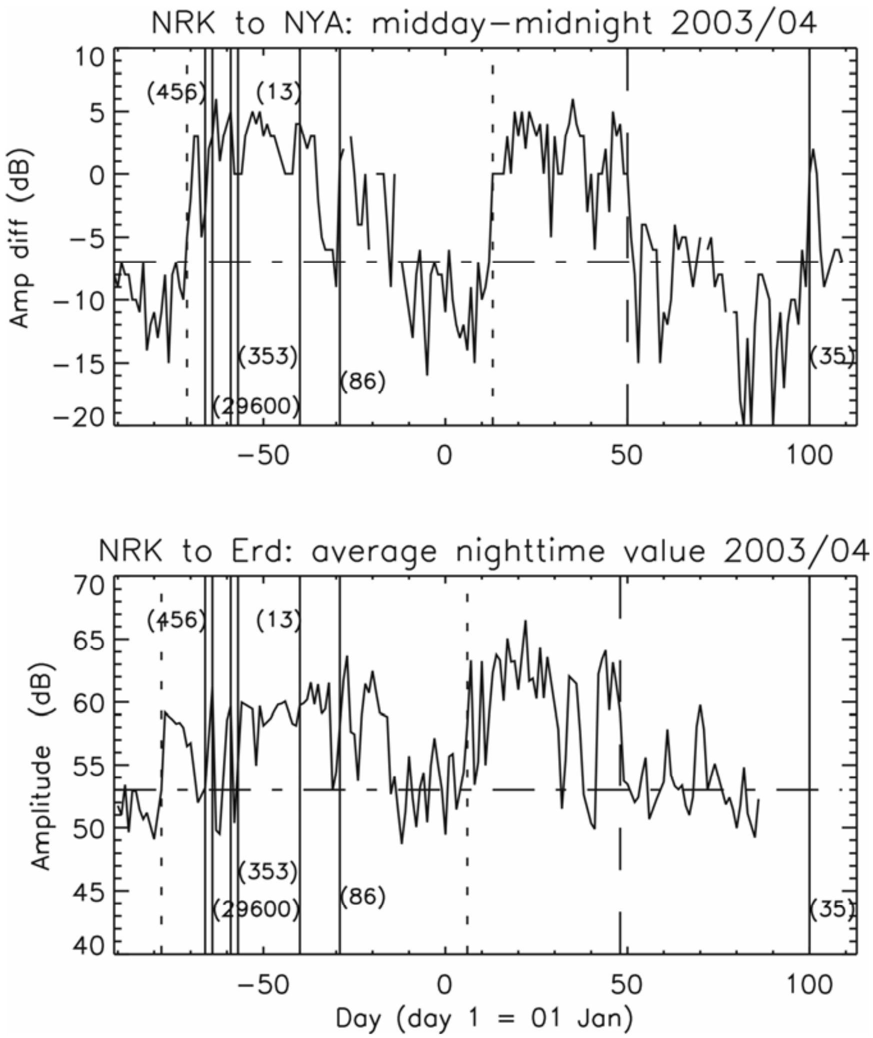

Figure 7. The winter-time average nighttime amplitude for the Iceland transmitter received at Érd, Hungary, during winter–time 2003-04 compared with the NRK to Ny Ålesund difference amplitude for the same period. The horizontal and vertical lines are as Figure 2 where the peak particle flux units (pfu) are given in parentheses plotted close to the vertical solid lines, with the addition of long-dashed vertical lines showing the end of the descent of NO_X in February 2004.

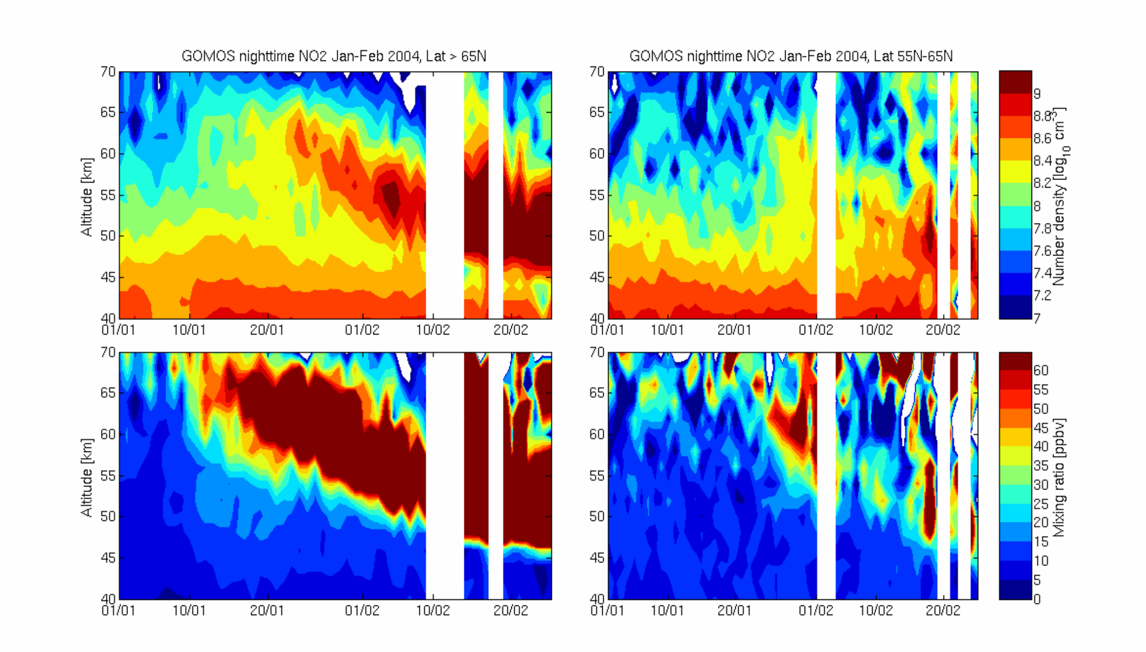

Figure 8. (Left top) The GOMOS nighttime NO_2 number density for latitudes >65°N during the period January and February 2004. (Left bottom) The NO_2 mixing ratio over the same period. (Right top) The NO_2 number density for latitudes 55-65°N from January and February 2004. (Right bottom) The NO_2 mixing ratio over the same period. The nighttime NO_2 measurements are used as an estimation of the total NO_X ($NO + NO_2$).

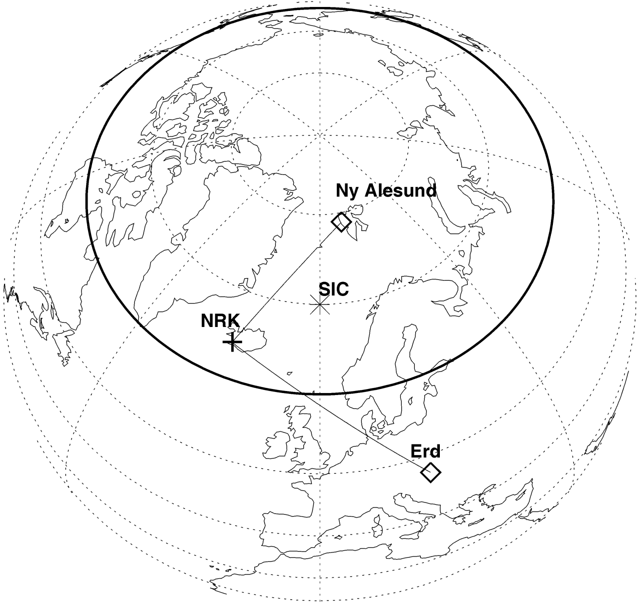
Ny Alesund
SIC
NRK
Erd

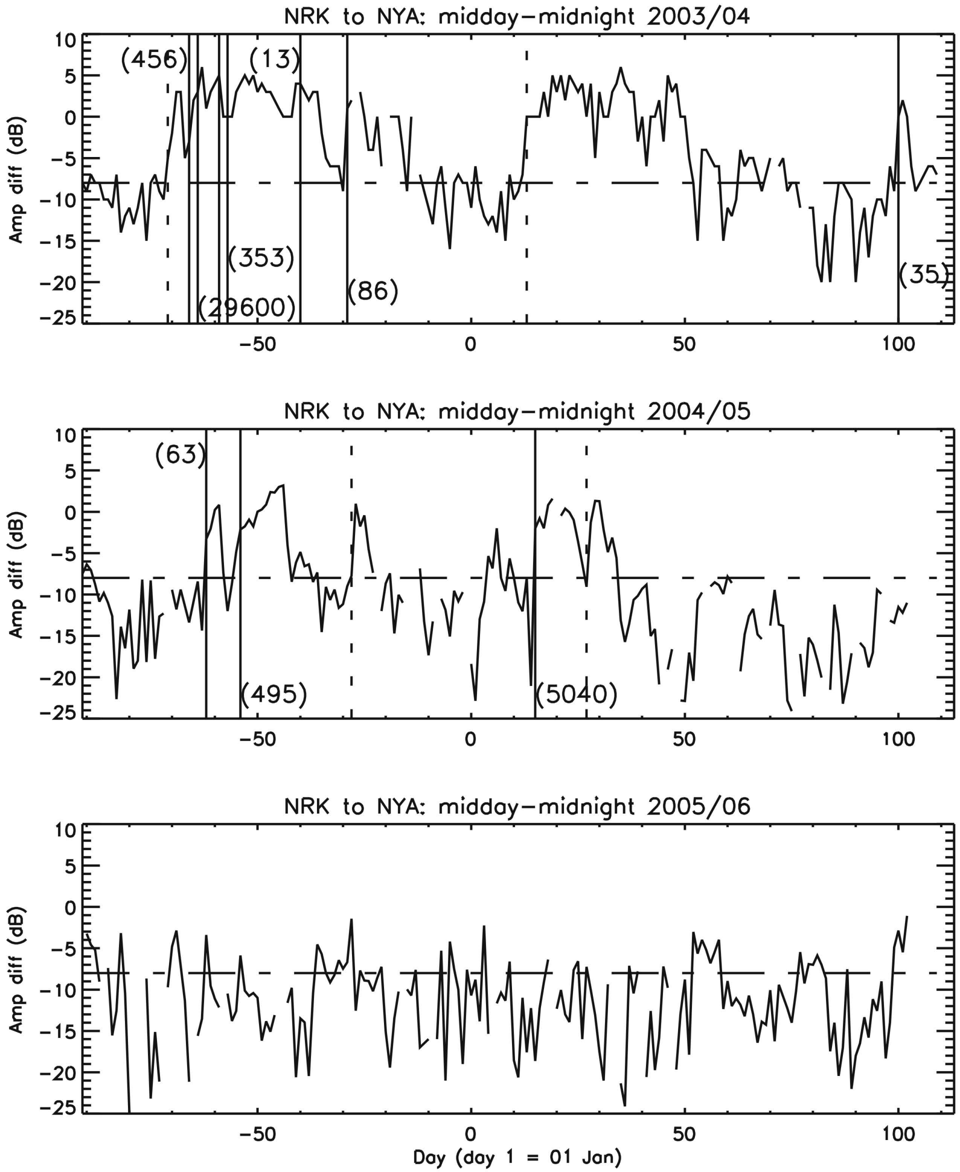
NRK to NYA: midday−midnight 2003/04
Amp diff (dB)
(456)
(13)
(353)
(29600)
(86)
(35)
NRK to NYA: midday−midnight 2004/05
Amp diff (dB)
(63)
(495)
(5040)
NRK to NYA: midday−midnight 2005/06
Amp diff (dB)
Day (day 1 = 01 Jan)

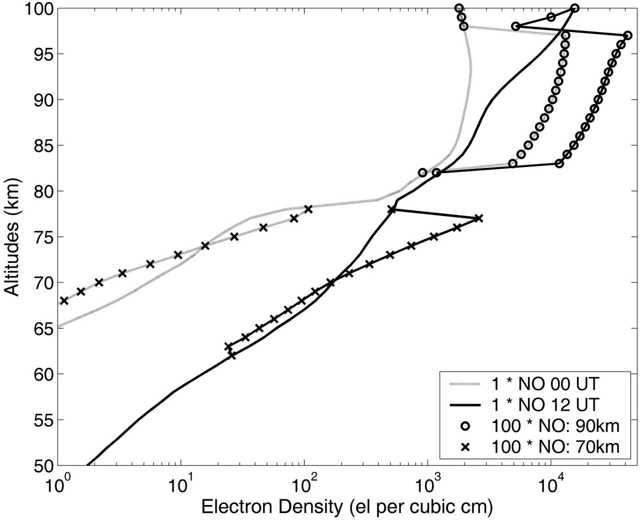

Altitudes (km)
Electron Density (el per cubic cm)
1 * NO 00 UT
1 * NO 12 UT
100 * NO: 90km
100 * NO: 70km

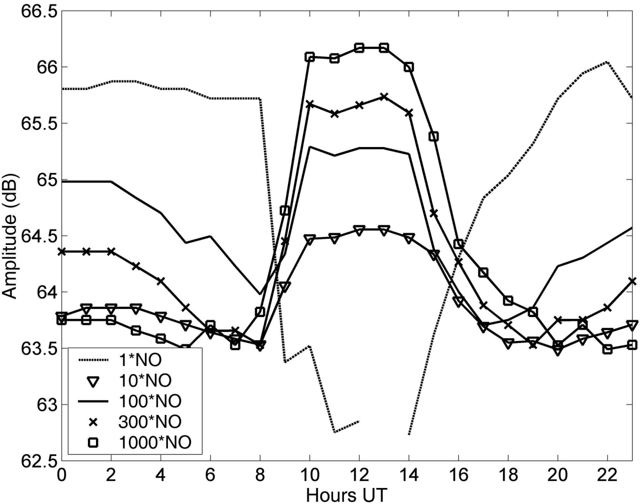

66.5
66
65.5
65
64.5
64
63.5
63
62.5
Amplitude (dB)
0
2
4
6
8
10
12
14
16
18
20
22
Hours UT
1*NO
10*NO
100*NO
300*NO
1000*NO

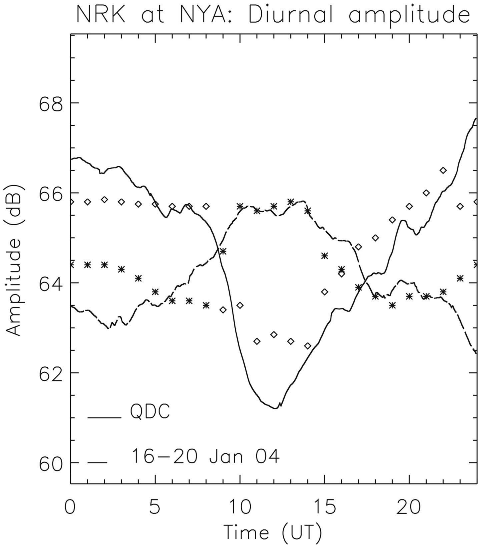
NRK at NYA: Diurnal amplitude
Amplitude (dB)
Time (UT)
QDC
16–20 Jan 04
60
62
64
66
68
0
5
10
15
20

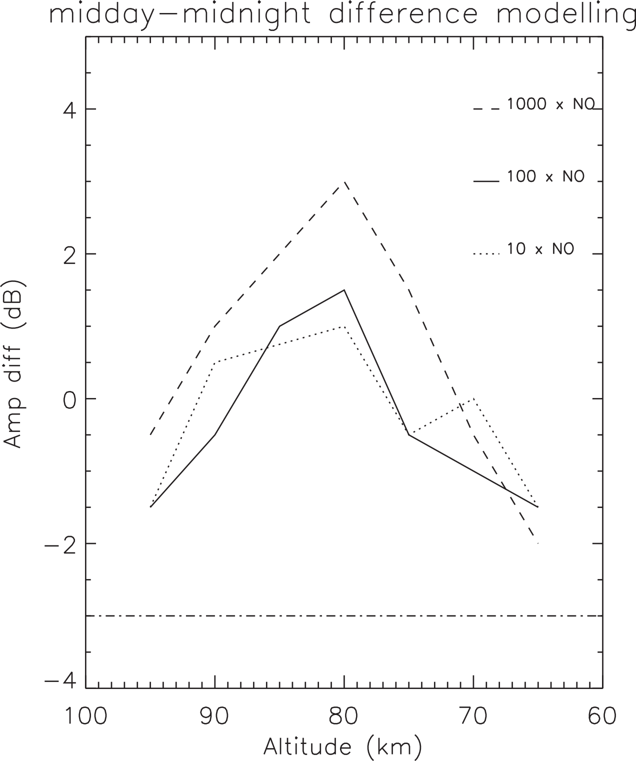

midday−midnight difference modelling
1000 x NO
100 x NO
10 x NO
Amp diff (dB)
Altitude (km)
4
2
0
−2
−4
100
90
80
70
60

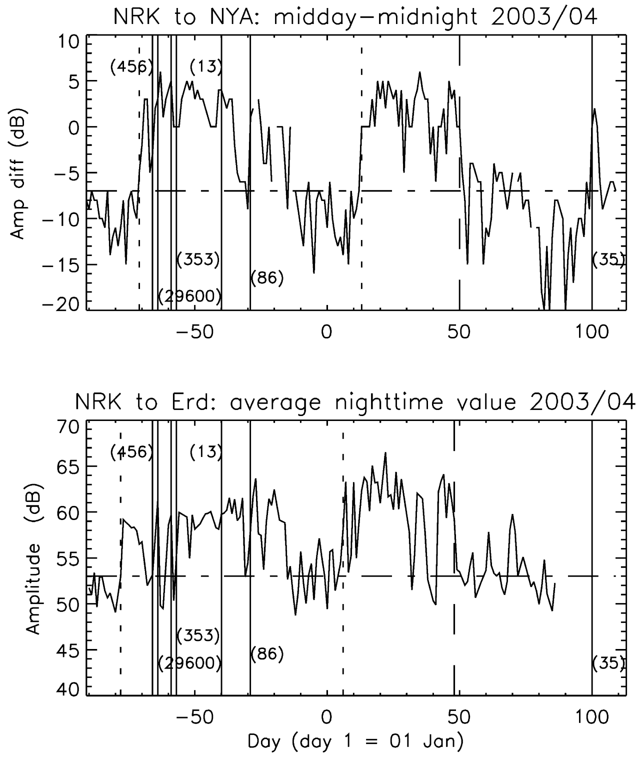

NRK to NYA: midday−midnight 2003/04
Amp diff (dB)
(456)
(13)
(353)
(29600)
(86)
(35)
NRK to Erd: average nighttime value 2003/04
Amplitude (dB)
(456)
(13)
(353)
(29600)
(86)
(35)
Day (day 1 = 01 Jan)

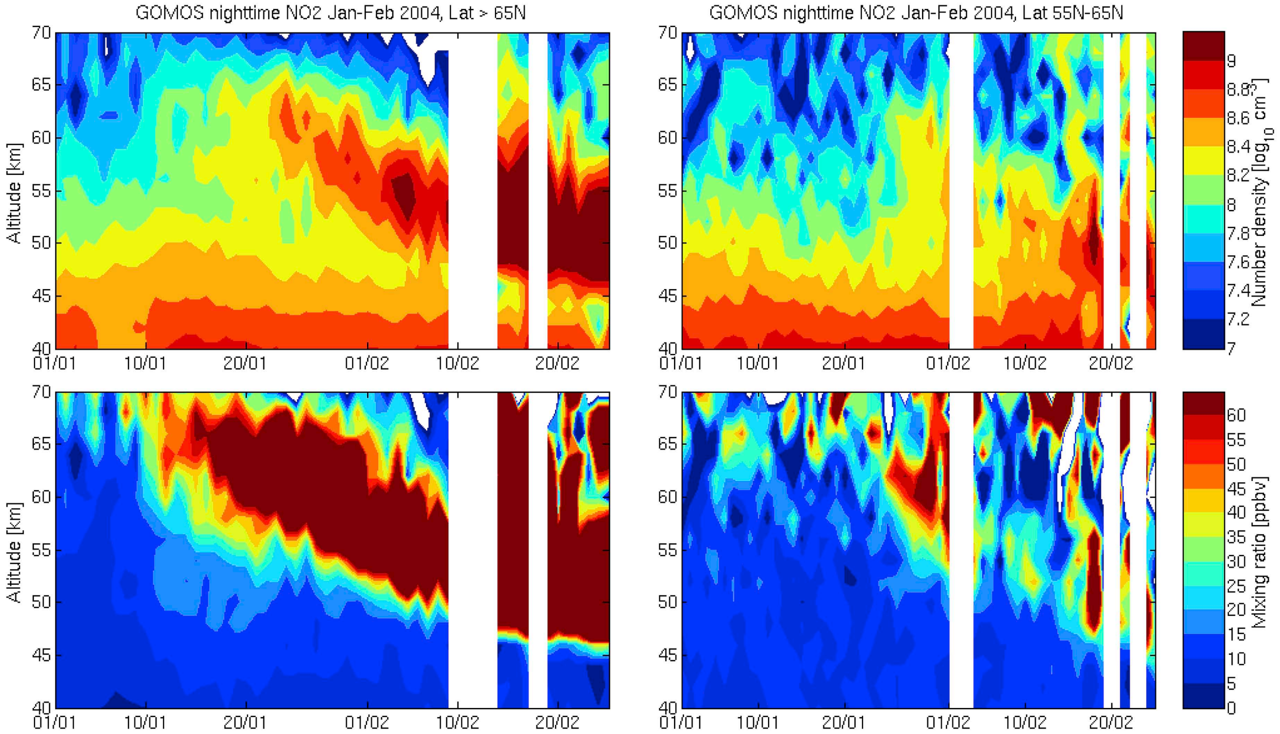

GOMOS nighttime NO2 Jan-Feb 2004, Lat > 65N
GOMOS nighttime NO2 Jan-Feb 2004, Lat 55N-65N
Altitude [km]
70
65
60
55
50
45
40
01/01
10/01
20/01
01/02
10/02
20/02
Number density [log10 cm-3]
9
8.8
8.6
8.4
8.2
8
7.8
7.6
7.4
7.2
7
Mixing ratio [ppbv]
60
55
50
45
40
35
30
25
20
15
10
5
0